Nanotechnology **19** (2008) 455704 (5pp) doi:10.1088/0957-4484/19/45/455704

Identification and control of the origin of photoluminescence from silicon quantum dots

H L Hao and W Z Shen[1]

Laboratory of Condensed Matter Spectroscopy and Opto-Electronic Physics, Department of Physics, Shanghai Jiao Tong University, 1954 Hua Shan Road, Shanghai 200030, People's Republic of China

E-mail: wzshen@sjtu.edu.cn

Received 1 August 2008, in final form 8 September 2008
Published 9 October 2008
Online at stacks.iop.org/Nano/19/455704

Abstract

We present a detailed investigation into the origin of photoluminescence (PL) from silicon quantum dots in hydrogenated amorphous silicon nitride annealed in oxygen ambient. On the basis of structural characterization, temperature-dependent PL, time-resolved PL, and PL excitation spectra, we identify that the luminescence of the oxidized samples originates from the localized exciton radiative recombination via the surface states related to Si–N or Si–O–Si bonds. In combination with the results due to annealing in argon and hydrogen environments, we have further shown that control of the origin of the PL can be realized by modifying the radiative defect density through annealing treatment.

Silicon quantum dots (Si QDs) embedded in hydrogenated amorphous silicon nitride (α-SiN$_x$:H) films represent good candidates for Si-based light-emitting devices due to the relatively low barrier (~2.0 eV) for carriers. Park *et al* [1] have achieved intensive visible light emissions with different wavelengths originating from the quantum confinement effect (QCE) by controlling the Si QD size. Although extensive work on the light emission properties of Si QDs has been done, the exact mechanism for the photoluminescence (PL) still remains controversial. It is generally accepted that the QCE and highly localized interface states between Si and silicon nitride play important roles in the light emission related to Si QDs, both of them being size dependent [2, 3].

Recently, we have demonstrated [4] that, when annealing α-SiN$_x$:H in inert argon ambient, the luminescence from Si QDs of small size is dominated by a QCE with annealing temperature (T_A) below/at 800 °C, while the PL mechanism changes to interface state assisted radiative recombination with further increase of T_A due to the coalescence, overgrowth, and expansion of Si QDs. Godefroo *et al* [5] have reported that the PL from Si QDs annealed in active hydrogen ambient originates mainly from the QCE due to the drastically decreased defect density, and the light emission mechanism has been converted to radiative defect states by using ultraviolet illumination to drive out the hydrogen (i.e., reintroduce the defects).

The changeable radiative recombination characteristics of Si QDs in different annealing environments not only provide ways to identify the PL mechanism, but also realize the possibility to control the origin of the luminescence. Compared with argon and hydrogen, oxygen is more active and it can react easily with both Si and N, resulting in a more complicated α-SiN$_x$:H network. In this study, we have carried out a detailed investigation of the PL of Si QDs annealed in oxygen ambient, and we present a clear luminescence mechanism picture for Si QDs in silicon nitride in combination with the results in argon and hydrogen environments.

The deposition process for the α-SiN$_x$:H thin films studied has been described elsewhere [4]. The samples, grown at a temperature of 300 °C, were annealed at a temperature T_A of 500–1100 °C for 30 min in oxygen ambient. PL and Raman scattering spectra were obtained on a Jobin–Yvon LabRAM HR 800 UV micro-Raman spectrometer using the 514.5 nm line of an Ar^+ laser and the 325.0 nm line of a He–Cd laser, respectively. The bonding environments and chemical compositions were analyzed by infrared absorption spectra (using a Nicolet Nexus 870 Fourier transform infrared spectrometer) and PHI Quantum 2000 x-ray photoelectron spectroscopy (XPS) with an Al Kα x-ray excitation source

[1] Author to whom any correspondence should be addressed.

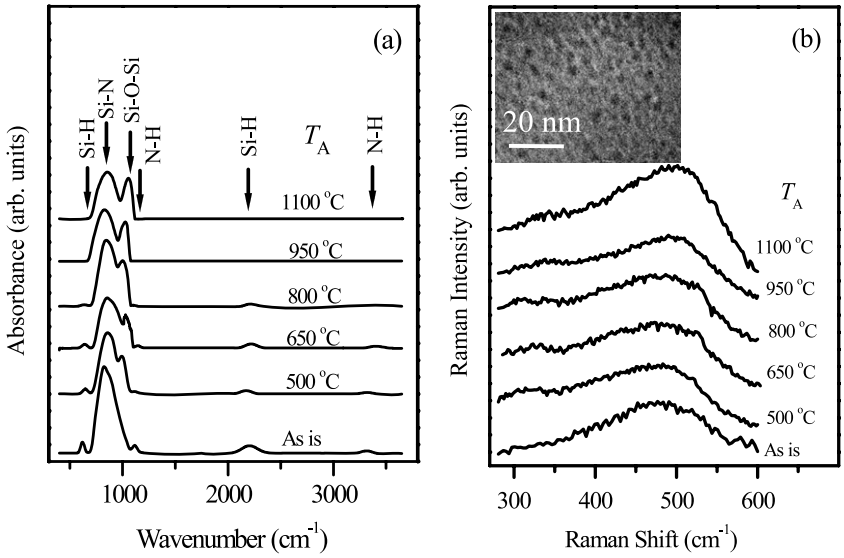

Figure 1. Room-temperature (a) infrared absorption spectra and (b) Raman spectra of oxidized samples under different annealing temperatures T_A. The inset shows the cross-sectional HRTEM image of α-Si QDs with $T_A = 500\,^{\circ}C$.

($h\nu = 1486.6$ eV). PL excitation (PLE) spectra were recorded by an Edinburgh Instruments FLS920 spectrometer through normalizing the variation in the Xe lamp output over the spectral range of interest. Time-resolved PL was measured by using a 405.0 nm diode laser with a pulse width of 60.0 ps as the excitation source.

Figure 1(a) presents the infrared absorption spectra of the oxidized samples and an as-deposited sample for comparison, which can reveal the direct structural information through the evolvement of the chemical bonds with the oxidized temperature T_A inside the α-SiN_x:H thin films. The absorption bands at ~610, 830, 1100, 2220, and 3320 cm^{-1} can be assigned to the modes of Si–H bending, asymmetric Si–N stretching, N–H rocking, Si–H stretching, and N–H stretching, respectively [6]. With the increase of T_A, the hydrogen (Si–H and N–H) bonds decrease gradually and disappear at 950 °C, where the hydrogen effuses completely from the α-SiN_x:H thin films. In contrast to the as-deposited sample, an absorption peak at about 960–1056 cm^{-1} can be observed in the oxidized samples under different T_A, which can be attributed to the Si–O–Si stretching vibration [7]. The peak position of the Si–O–Si bond shifts progressively toward higher energy with T_A, accompanied with an increase of the intensity, indicating that the oxidation is enhanced at elevated annealing temperature [8]. At the same time, the intensity of the Si–N bond peak decreases continuously with increasing T_A, as expected from the strong oxidation at high T_A [9].

The corresponding Raman spectra are shown in figure 1(b). The Raman peak falls in the range from ~482 to 498 cm^{-1}, which is a typical Raman characteristic of α-Si QDs [4, 6]. With increasing T_A, the peak shifts toward higher energy and the full width at half maximum (FWHM) becomes narrower, indicating an increase of the size of the α-Si QDs [10]. High resolution transmission electron microscopy (HRTEM, JEOL JEM-2100F) measurements can directly confirm the existence and state of the Si QDs. The inset of figure 1(b) is a cross-sectional HRTEM micrograph of Si QDs embedded in the α-SiN_x:H sample with $T_A = 500\,^{\circ}C$. Due to the higher density than that of the amorphous silicon nitride matrix, the Si QDs appear as dark spots, and the average dot size is about 3.3 nm. It is noted that no lattice fringes can be found, suggesting that these Si QDs are amorphous, in agreement with the Raman results. The mechanism of the formation and evolution of the α-Si QDs can be revealed from the infrared absorption observation shown in figure 1(a). During the annealing process of the α-SiN_x:H thin films, Si–H bonds are easily broken to provide the silicon nuclei for the formation of Si QDs at high T_A. The α-Si QDs formed will aggregate and grow with increasing T_A, resulting in the increase of the α-Si QD size (~4.9 nm at $T_A = 1100\,^{\circ}C$).

The modification of the composition in these α-SiN_x:H films can be explored by XPS measurements. Figure 2 displays the XPS spectra of Si 2p, N 1s, and O 1s photoelectron emission peaks taken at the surfaces of the films. The binding energy values were calibrated by using the value of contaminant carbon (C 1s = 284.8 eV) as a reference. In the as-deposited thin film, the broad Si 2p peak located at ~100.6 eV corresponds to the mixture of subnitride species in silicon nitride films. We have employed the random bonding model for the analysis of the bonding configurations, where the α-SiN_x network is considered as a statistical distribution of Si–$Si_{4-n}N_n$ (dotted curves) [4]. The appearance of the peak around 99.5 eV ($n = 0$) clearly indicates the existence of pure Si, though the pure Si 2p component is not very strong as a result of relative lower content of pure Si in silicon nitride films. Due to the higher electronegativity of oxygen than that of nitrogen, the Si 2p peak in silicon oxynitride has a higher binding energy in comparison to that in silicon nitride [11], resulting in the experimental fact that the strong Si 2p peak shifts to the high binding energy side with increasing T_A. When T_A reaches 1100 °C, the main peak at 103.2 eV and weak shoulder at around 101.5 eV correspond to the Si 2p peak in silicon oxynitride and silicon nitride, respectively [12]. Meanwhile, we can also observe that the relative intensity of

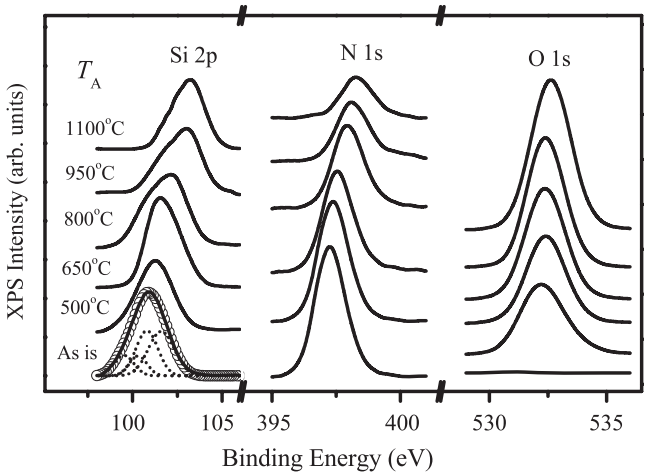

Figure 2. Si 2p, N 1s, and O 1s XPS spectra for the same samples as in figure 1, together with the experimental (solid curve) and calculated (open circles) Si 2p core-level binding energy of the as-deposited sample.

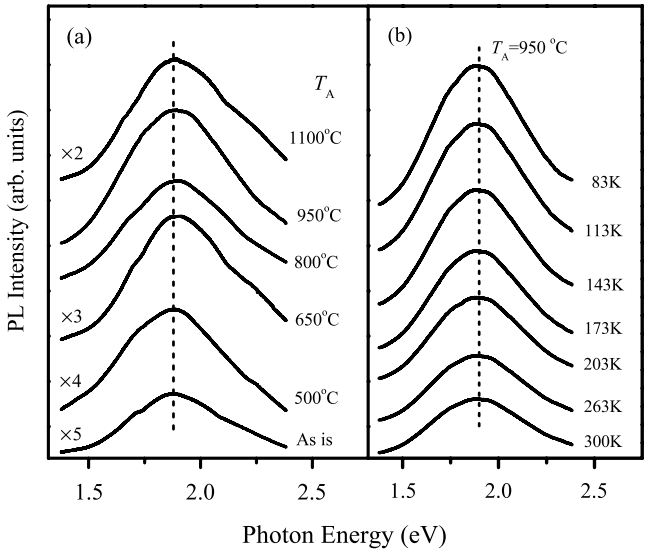

Figure 3. (a) Room-temperature PL spectra for the same samples as in figure 1. (b) Temperature-dependent PL spectra of the oxidized sample annealed at 950 °C.

the Si 2p peak in silicon oxynitride increases with T_A, which is consistent with the expectation for the enhanced oxidation of the films at higher T_A [13].

Due to the O–N induction effect [13] and/or upward shift of the Fermi level in silicon nitride [11], the higher oxygen concentration at higher T_A in the silicon oxynitride films would lead to the increase of the average binding energy of nitrogen atoms. As a result, the N 1s peak exhibits a large chemical shift from 397.2 eV in the as-deposited film to 398.3 eV in the oxidized sample at 1100 °C. At the same time, the nitrogen content would be reduced by a displacement reaction of oxidation in the films [13]; the N 1s peak intensity is found to decrease drastically with increasing heat treatment temperature. In the O 1s XPS spectra, it is clear that no oxygen has been detected on the surface of the as-deposited film. After oxidation treatment, a rapid increase of the O 1s peak intensity can be observed, together with a slight shift toward high energy from 532.1 eV in the sample annealed at 500 °C to 532.8 eV in the one annealed at 1100 °C. According to the charge transfer model [11], such a shift is also expected to be due to the fact that the Fermi level shifts toward the high energy level, demonstrating directly that the α-SiN$_x$:H film has been significantly oxidized at high T_A.

Figure 3(a) shows the room-temperature PL spectra of the α-SiN$_x$:H thin films annealed in oxygen ambient under different T_A, together with the as-deposited spectrum for comparison. It is found that, with the increase of T_A, the emission peak centered at 1.9 eV remains unchanged, while for the case of the α-SiN$_x$:H annealed in argon ambient, the PL peak exhibits a continuous redshift with the increase of T_A [5]. Simultaneously, the FWHM of the PL spectra increases from 0.49 eV in the as-deposited sample to 0.57 eV in the one with $T_A = 1100$ °C. We can also observe a significant improvement of the emission intensity for the oxidized samples over the as-deposited sample; the maximum PL intensity is obtained in the thin film annealed at $T_A = 950$ °C. With further increasing T_A to 1100 °C, the luminescence intensity starts to decrease: the integrated PL intensity of the sample annealed at $T_A = 950$ °C is about 2.4 times as large as that of the 1100 °C sample. It should be noted that the PL intensity of the oxidized films is remarkably enhanced compared with the samples annealed in argon ambient, indicating that moderate oxidation (confirmed by XPS analysis) is useful to achieve strong PL from silicon nitride films.

For the as-deposited sample, we have confirmed that the red luminescence at ∼1.90 eV originates from the QCE [4, 6]. To investigate the PL mechanism of the oxidized films, we first performed temperature-dependent PL measurements. Figure 3(b) presents the typical results for the film with $T_A = 950$ °C, where both the PL peak energy and FWHM are almost independent of temperature throughout the measured range. The temperature-dependent PL peak would have a blueshift due to the increasing energy gap of SiN$_x$:H with decreasing temperature, provided that the PL is related to the band-to-band recombination in Si QDs. Furthermore, the room-temperature PL peak energy is also found to be independent of T_A in figure 3(a), while the Si QD size increases with T_A, as revealed in the Raman spectra of figure 1(b). These observations suggest that the mechanism of light emission in the oxidized samples is not determined by the size-dependent QCE.

In order to clarify the light emission mechanism of the oxidized samples, we have further carried out time-resolved PL and PLE measurements. Figure 4(a) presents the experimental (open circles) and calculated (solid curves) decay results for the oxidized films. The decay process can be accurately fitted by a double exponential function, where the faster decay component increases from 0.80 to 0.93 ns, and the longer decay one from 1.73 to 4.70 ns with the increase of T_A. When the surface of Si QDs is oxidized (see figure 2), the Si=O bonds will introduce localized states in the band gap of the Si QDs [8]. First-principle calculations of the optical properties of Si QDs have revealed that the nanosecond decay time can be attributed to the localized state exciton transitions at the surfaces of the Si

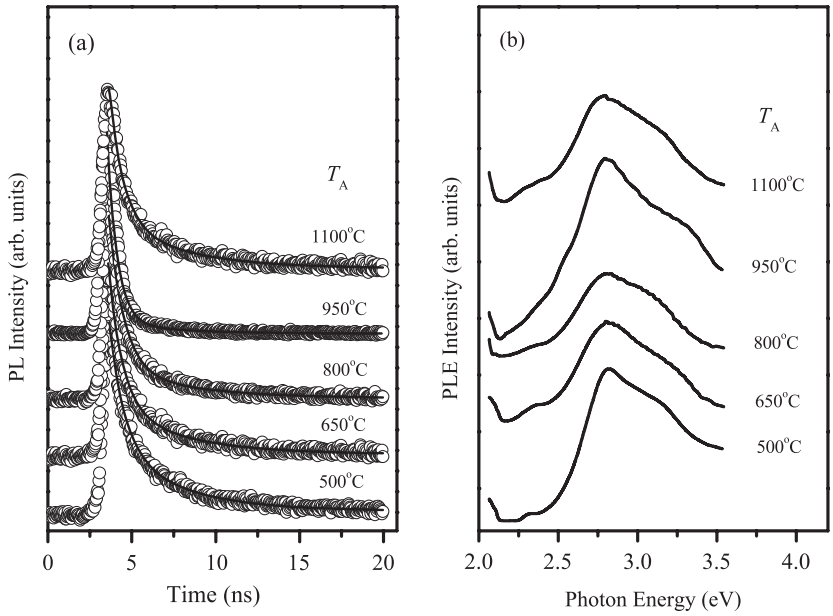

Figure 4. (a) Time-resolved PL spectra and (b) the corresponding PLE spectra monitored at 1.9 eV for the oxidized samples under different annealing temperatures T_A.

QDs, where the faster and longer decay components correlate to the nonradiative excitons' trapping time on the localized states and the recombination (both radiative and nonradiative) of the trapped excitons, respectively [14]. Figure 4(b) displays the PLE spectra of all the oxidized films with the detection energy of ∼1.90 eV. The PLE peak positions at 2.82 eV are independent of T_A, and smaller than the optical band gap (3.29 eV) of the samples [6], which suggests that the transition mainly occurs within the band gap. Compared with the PL peak energy, the PLE peak has a large Stokes shift of 0.92 eV for all the oxidized samples, indicating that the carriers are generated mostly in the energy level of 2.82 eV and then transferred to the localized states at the surface of the Si QDs [15].

We now focus on the radiative recombination process of the localized state excitons. It is usual to employ the configuration coordinate model to describe the larger Stokes shift and the broadening of the luminescence spectra in α-SiN_x:H thin films [15, 16]. In this model, the coupling between the electronic state and the lattice occurs through transverse acoustic phonons with a single frequency Ω, and the Stokes shift has the form $E_S = A^2/(M\Omega^2)$, with A a constant and M the mass of the coupling phonon. The coupling phonon energy can be expressed as $\hbar\Omega = W^2|_{T\to 0}/(4\ln 2)E_S$, where W is the FWHM of the PL spectrum, and it remains unchanged over the investigated temperature range in figure 3(b). The phonon energy $\hbar\Omega$ of the oxidized samples is found to increase continuously from 0.110 eV in the sample annealed at 500 °C to 0.132 eV in the sample with $T_A = 1100$ °C, all much larger than the room-temperature thermal energy of 0.026 eV. Moreover, the energies of 0.110 eV (887 cm^{-1}) and 0.132 eV (1056 cm^{-1}) correspond well to the Si–N and Si–O–Si stretching vibration frequencies, respectively, which indicates that the PL mechanism is related to the electron–hole pair recombination associated with Si–N or Si–O–Si vibration phonons. On the basis of these arguments, we conclude that the luminescence of the oxidized samples originates from the localized exciton radiative recombination via the surface states of the Si QDs related to the Si–N or Si–O–Si bonds.

The above observations also establish an experimental basis for better understanding the significant improvement of the PL intensity with oxidation treatment under $T_A \leqslant 950$ °C. With increasing T_A, some defects acting as nonradiative recombination centers in the α-SiN_x:H thin film network can be effectively passivated. The reduced interface defects with increasing T_A make the interfaces between silicon and silicon oxynitride smoother and more conducting to oxygen, leading to the generation of a large number of luminescent centers [9]. The PL intensity η_i can be expressed as a function of the radiative carrier lifetime (τ_r) and the nonradiative lifetime (τ_{nr}): $\eta_i = 1/(1 + \tau_r/\tau_{nr})$ [17]. τ_r remains almost unchanged, while the nonradiative recombination rate is remarkably decreased (the increase of τ_{nr}) with the defect density; therefore higher PL intensity is expected at higher T_A. Nevertheless, the number of Si–N bonds decreases drastically at very high T_A (see figure 1(a)), corresponding to the rapid reduction of the nitrogen content in figure 2, where the interface between silicon and silicon oxynitride cannot be effectively passivated. As a result, fewer photoexcited carriers can be transferred to the PL emission centers, and the PL intensity will be reduced at very high T_A (1100 °C).

After the detailed investigation of PL properties for Si QDs annealed in oxygen ambient, we are able to present further a clear luminescence mechanism picture of the Si QDs by the aid of the reported results under different annealing environments. Annealing in inert argon ambient is a process of thermal relaxation: the PL origin changes from QCE at low T_A to interface states at high T_A due to the high interface state density induced by the large-size Si QDs [4]. In a hydrogen environment, annealing treatment can drastically reduce the

radiative defect density, which would make QCE dominant in the PL [5]. Nevertheless, by annealing in active oxygen ambient, more localized surface states will be introduced due to the oxidation of the Si QD surfaces, leading to the localized surface state related light emission. It is clear that the structure and surface chemistry of the Si QDs determine the nature of the luminescence, and annealing treatment in different environments is therefore a simple and effective technique to control the origin of the PL in Si QDs from QCE to localized interface/surface states and vice versa via the radiative defect density.

In summary, we have performed an overall study on the origin of the visible PL from Si QDs annealed in oxygen ambient. Infrared absorption and XPS measurements demonstrate that the oxidation of the α-SiN_x:H films is enhanced at elevated temperature. Through analyzing the temperature-dependent PL, time-resolved PL, and PLE spectra, we attribute the luminescence to localized exciton radiative recombination via the surface states of the Si QDs related to the Si–N or Si–O–Si bonds. In combination with the PL mechanisms from Si QDs annealed in argon and hydrogen environments, it is suggested that the control of the origin from QCE to interface/surface state related recombination can be realized by different annealing treatments to modify the radiative defect density.

Acknowledgments

This work was supported by the Natural Science Foundation of China under contracts 10674094 and 10734020, National Major Basic Research Project of 2006CB921507, National Minister of Education Program of IRT0524, and Shanghai Municipal Key Projects of 06JC14039 and 08XD14022.

References

[1] Park N-M, Choi C-J, Seong T-Y and Park S-J 2001 *Phys. Rev. Lett.* **86** 1355
[2] Wang X X, Zhang J G, Ding L, Cheng B W, Ge W K, Yu J Z and Wang Q M 2005 *Phys. Rev.* B **72** 195313
[3] Hadjisavvas G and Kelires P C 2004 *Phys. Rev. Lett.* **93** 226104
[4] Hao H L, Wu L K and Shen W Z 2008 *Appl. Phys. Lett.* **92** 121922
[5] Godefroo S, Hayne M, Jivanescu M, Stesmans A, Zacharias M, Lebedev O I, Tendeloo G V and Moshchalkov V V 2008 *Nat. Nanotechnol.* **3** 174
[6] Hao H L, Wu L K, Shen W Z and Dekkers H F W 2007 *Appl. Phys. Lett.* **91** 201922
[7] Kohli S, Theil J A, Dippo P C, Jones K M, Jassim M M, Ahrenkiel R K, Rithner C D and Dorhout P K 2004 *Nanotechnology* **15** 1831
[8] Wang M H, Yang D R, Li D S, Yuan Z Z and Que D L 2007 *J. Appl. Phys.* **101** 103504
[9] Xu M, Xu S, Chai J W, Long J D, Cheng Q J, Ee Y C and Ostrikov K 2008 *J. Appl. Phys.* **103** 053512
[10] Wang Y Q, Wang Y G, Cao L and Cao Z X 2003 *Appl. Phys. Lett.* **83** 3474
[11] Hasegawa S, He L, Inokuma T and Kurata Y 1992 *Phys. Rev.* B **46** 12478
[12] Cova P, Poulin S, Grenier O and Masut R A 2005 *J. Appl. Phys.* **97** 073518
[13] Jehanathan N, Liu Y, Walmsley B, Dell J and Saunders M 2006 *J. Appl. Phys.* **100** 123516
[14] Negro L D, Yi J H, Michel J, Kimerling L C, Chang T-W F, Sukhovatkin V and Sargent E H 2006 *Appl. Phys. Lett.* **88** 233109
[15] Yamaguchi K, Mizushima K and Sassa K 2000 *Appl. Phys. Lett.* **77** 3773
[16] Huang R, Chen K J, Qian B, Chen S, Li W, Xu J, Ma Z Y and Huang X F 2006 *Appl. Phys. Lett.* **89** 221120
[17] Kwack H-S, Sun Y P, Cho Y-H, Park N-M and Park S-J 2003 *Appl. Phys. Lett.* **83** 2901